Multi-epoch spectroscopy of IYUMa: quiescence, rise, normal outburst and superoutburst

Mon. Not. R. Astron. Soc. **357,** 69–81 (2005) doi:10.1111/j.1365-2966.2005.08639.x

Multi-epoch spectroscopy of IY UMa: quiescence, rise, normal outburst and superoutburst

Daniel J. Rolfe,[1,2] Carole A. Haswell,[1⋆] Timothy M. C. Abbott,[3,4] Luisa Morales-Rueda,[5,6] T. R. Marsh[5,7] and G. Holdaway[5,8]

[1]*Department of Physics & Astronomy, The Open University, Walton Hall, Milton Keynes MK7 6AA*
[2]*Department of Physics & Astronomy, University of Leicester, University Road, Leicester LE1 7RH*
[3]*Cerro Tololo Inter-American Observatory, Casilla 603, La Serena, Chile*
[4]*Nordic Optical Telescope, Roque del Los Muchachos & Santa Cruz de La Palma, Canary Islands, Spain*
[5]*Department of Physics & Astronomy, Southampton University, Southampton SO17 1BJ*
[6]*Department of Astrophysics, University of Nijmegen, PO Box 9010, 6500 GL Nijmegen, the Netherlands*
[7]*Department of Physics, University of Warwick, Coventry CV4 7AL*
[8]*Fault Studies & Fuel Branch, British Energy Generation Ltd, Gloucester GL4 3RS*

Accepted 2004 October 28. Received 2004 October 25; in original form 2004 January 23

ABSTRACT

We exploit rare observations covering the time before and during a normal outburst in the deeply eclipsing SU UMa system IY UMa to study the dramatic changes in the accretion flow and emission at the onset of outburst. Through Doppler tomography we study the emission distribution, revealing classic accretion flow behaviour in quiescence, with the stream–disc impact ionizing the nearby accretion disc. We observe a delay of hours to a couple of days between the rise in continuum and the rise in the emission lines at the onset of the outburst. From line profiles and Doppler maps during normal and superoutburst, we conclude that reprocessing of boundary layer (BL) radiation is the dominant emission line mechanism in outburst and that the normal outburst began in the outer disc. The stream–disc impact feature (the orbital hump) in the Hα line flux light curve disappears before the onset of the normal outburst and may be an observable signal heralding an impending outburst.

Key words: techniques: spectroscopic – stars: dwarf novae – stars: individual: IY UMa – novae, cataclysmic variables.

1 INTRODUCTION

IY UMa is an SU UMa type dwarf nova cataclysmic variable (CV). These are systems in which a white dwarf accretes via Roche lobe overflow from the donor, forming an accretion disc around the white dwarf, which undergoes a series of short normal outbursts ($\sim$5 d for IY UMa) and longer superoutbursts ($\sim$ 3 weeks). The outbursts are thought to result from the switching of the disc between a cool, neutral, low-viscosity state and a hot, ionized, viscous state. In the cool state very little mass is transferred inwards, while in the hot state mass is rapidly accreted on to the white dwarf. Superoutbursts are thought to differ from normal outbursts as a result of the onset of a tidal instability in the disc, in which a 3:1 resonance between tidal forces and orbits of particles in the disc leads to a distorted, precessing disc. Periodic luminosity modulations, called superhumps, with periods a few per cent longer than the orbital period are the defining characteristic of superoutbursts. Superhumps result from the interaction of the donor orbit with the eccentric disc. For a review see Osaki (1996) and for a recent discussion Osaki & Meyer (2003).

⋆E-mail: C.A.Haswell@open.ac.uk

Patterson et al. (2000, hereafter P2000) and Rolfe, Haswell & Patterson (2001b) present detailed photometric studies of the superoutburst and superhumps of IY UMa in 2000 January. Spectroscopic observations reveal: a bright hotspot and deep white dwarf absorption lines during quiescence (Rolfe, Abbott & Haswell 2001a; P2000); an eccentric disc during superoutburst (Wu et al. 2001); lines powered by reprocessed boundary layer (BL) emission during outburst (Rolfe, Abbott & Haswell 2002); and an M dwarf donor star (Rolfe 2002).

We present spectroscopic observations of IY UMa in quiescence, rise, outburst and superoutburst. Section 2 presents the observations. In Section 3, we discuss the average spectra epoch by epoch. We cover the light curves in Section 4, and the line profile variations and detailed accretion flow in Section 5. In Sections 6 and 7, we discuss and summarize our findings.

2 OBSERVATIONS AND DATA REDUCTION

Fig. 1 marks our observations in relation to the long-term light curve from the Variable Star Network (VSNET).

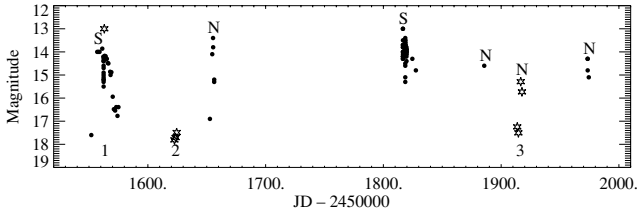

Figure 1. Variable Star Network (VSNET) observations of IY UMa outbursts (circles) and observing runs presented in this work (stars). S denotes a superoutburst, N a normal outburst. The observations are marked: 1 – William Herschel Telescope (WHT), 2000 January; 2 – Nordic Optical Telescope (NOT), 2000 March; and 3 – NOT, 2001 January.

Table 1. The observations. $\Delta\lambda$ is the FWHM spectral resolution, N is the number of spectra. The instrument column lists the grating, CCD and readout mode for the red and blue ISIS arms in William Herschel Telescope (WHT) observations and the grism number for the Nordic Optical Telescope (NOT) observations.

Tel. Date	Instr.	Orbits	N	Exp. (s)	λ range (Å)	$\Delta\lambda$ (Å)
WHT	ISIS					
19/1/00	R1200R Tek/Quick	1.4	64	80	6350–6750	0.8
	R1200B EEV/Std.	1.3	53	80	4270–5070	0.9
NOT	ALFOSC					
18/3/00	6	4.1	59	300	3180–5550	6
19/3/00	7	2.9	80	180	3820–6840	6
20/3/00	7	1.6	64	120	3820–6840	5
3/1/01	8	1.6	21	360	5810–8350	5
4/1/01	8	1.2	18	360	5810–8350	5
6/1/01	7	1.1	58	60	3820–6840	5
7/1/01	7	2.2	131	60	3820–6840	5

Orbital phases for all observations in this work were calculated using the white dwarf ephemeris in P2000.

2.1 WHT

On 2000 January 19, we used the ISIS double beam spectrograph on the 4.2-m William Herschel Telescope (WHT) on La Palma (see Table 1 for details) to monitor Hα and He I 6678 Å in the red arm and Hγ, Hβ, He II and several He I lines in the blue arm.

Standard CCD processing, optimal extraction of spectra (Marsh 1989), wavelength calibration, and instrumental response and extinction corrections were performed. Uncertainties on every point were propagated through every stage of the data reduction.

As we did not put a comparison star in the slit with IY UMa, the spectra have not been corrected for slit losses. This means that the variability seen from one spectrum to the next could be the result of passing clouds and it is most probably not the result of the intrinsic variability of the system.

2.2 NOT

The Nordic Optical Telescope (NOT) observations comprise approximately 14 binary orbits of spectra from 2000 March and 2001 January taken using the ALFOSC spectrograph (see Table 1).

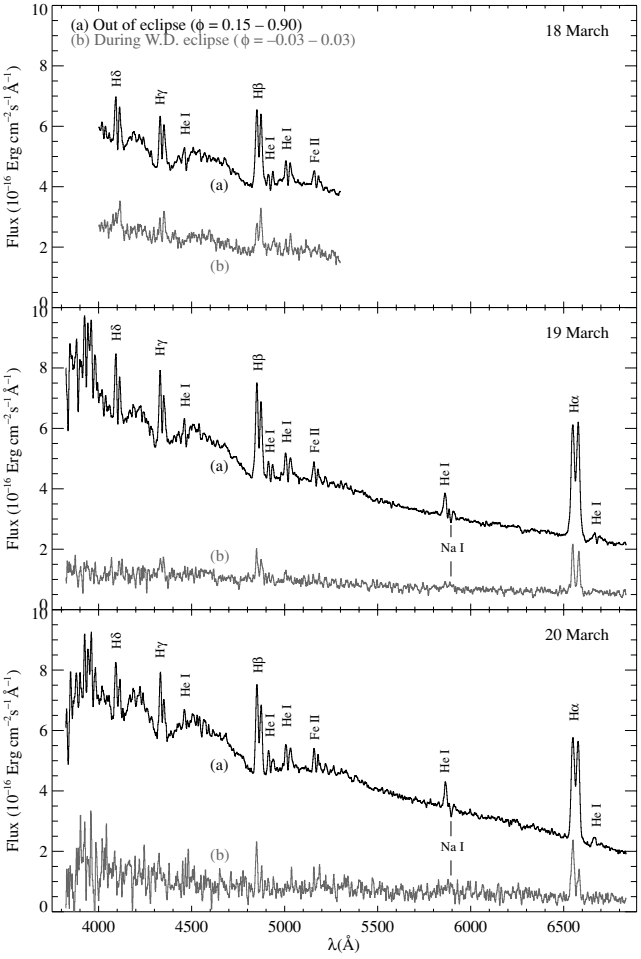

Figure 2. Average spectra of IY UMa during quiescence in 2000 March.

The 2000 March observations were reduced and flux calibrated following standard procedures without corrections for slit losses. The March 18 spectra are reliable only between approximately 4000 and 5200 Å as a result of wavelength calibration problems.

The 2001 January exposures of IY UMa included a nearby comparison star for correction of slit losses. Wide slit exposures of IY UMa and the comparison, and of a flux standard, were taken and used for flux and slit loss calibration.

The 2001 January observations were fully flux calibrated and slit loss corrected above ∼4800 Å and degraded only by the wavelength-dependent slit losses at shorter wavelengths.

3 AVERAGE SPECTRA

3.1 2000 March: IY UMa in quiescence

Fig. 2 shows 2000 March average nightly spectra during and outside eclipses (phase ranges given in Fig. 2). The spectra have been smoothed by slightly less than the instrumental resolution. Strong, double-peaked Balmer, He I and Fe II emission lines are superimposed on a blue continuum. Broad absorption wings are seen around the Balmer emission lines except Hα and there are deep cores between the double peaks of the lines, reaching below the continuum in some cases. Such features are seen in two other high-inclination dwarf novae in quiescence: Z Cha (Marsh, Horne & Shipman 1987)

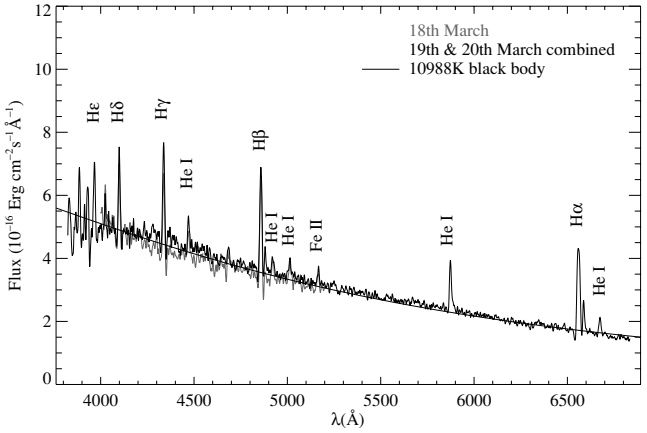

Figure 3. The spectrum of the orbital hump, obtained by subtracting the average spectrum at the hump minimum from the average at the hump maximum (smoothed as in Fig.2). The smooth curve is the blackbody fit.

and OY Car (Hessman et al. 1989). Weak Na I doublet absorption at 5890–5896 Å is superimposed on He I 5876 Å.

The full width of the Balmer absorption wings is approximately 20 000 km s^{-1}, far too large to be Doppler-shifted disc material. The broad absorption wings disappear during the white dwarf eclipse; we conclude that these features come predominantly from the white dwarf (cf. Marsh et al. 1987). The absorption cores remain during the white dwarf eclipse, indicating they arise at least partially in the disc.

3.1.1 The hotspot spectrum

The very high inclination of IY UMa (cf. Steeghs et al. 2003) leads to a prominent orbital hump as the hotspot comes into view. The hotspot spectra in Fig. 3 were produced by subtracting the average spectrum around the hump minimum (orbital phases 0.5 to 0.6) from that around the hump maximum (phases 0.75 to 0.9). Strong emission lines in the Balmer series and weaker emission in He I and Fe II are superimposed on a blue continuum. The lines show one strong peak indicating a concentrated emission region, with some weaker peaks and dips arising from changes in line profile between the hump maximum and minimum.

Fig 3 shows a simple blackbody spectrum fit (assuming $d = 190 \pm 60$ pc, from P2000), which has a temperature $T = 10990 \pm 120$ K and emitting area $A = 3.8^{+3.0}_{-2.1} \times 10^{18}$ cm^2 ($= 0.0015^{+0.0011}_{-0.0008}\, a^2$ where a is the orbital separation). The emission lines were masked out. The error in T is a 90 per cent confidence estimate where the confidence region was determined using a Monte Carlo bootstrap-type resampling and fitting of the data 30 000 times. The error in A is dominated by propagating the uncertainty in d. Systematic errors are not accounted for in these confidence limits, e.g. errors in the atmospheric extinction correction and any deviation of the real spectrum from the assumed blackbody form. The latter is hard to detect because we only sample the tail of the Rayleigh–Jeans distribution. Marsh et al. (1987) produced a hotspot spectrum for Z Cha using the same technique, finding a non-blackbody continuum, with a significant drop below 4000 Å, probably resulting from Balmer absorption. The effective area determined here is consistent with the simple stream–disc impact model used for IY UMa in Rolfe et al. (2001b). The temperature is typical: hotspot temperatures of ∼10 000–20 000 K were found by Wood et al. (1986), Robinson et al. (1995) and Stanishev et al. (2001).

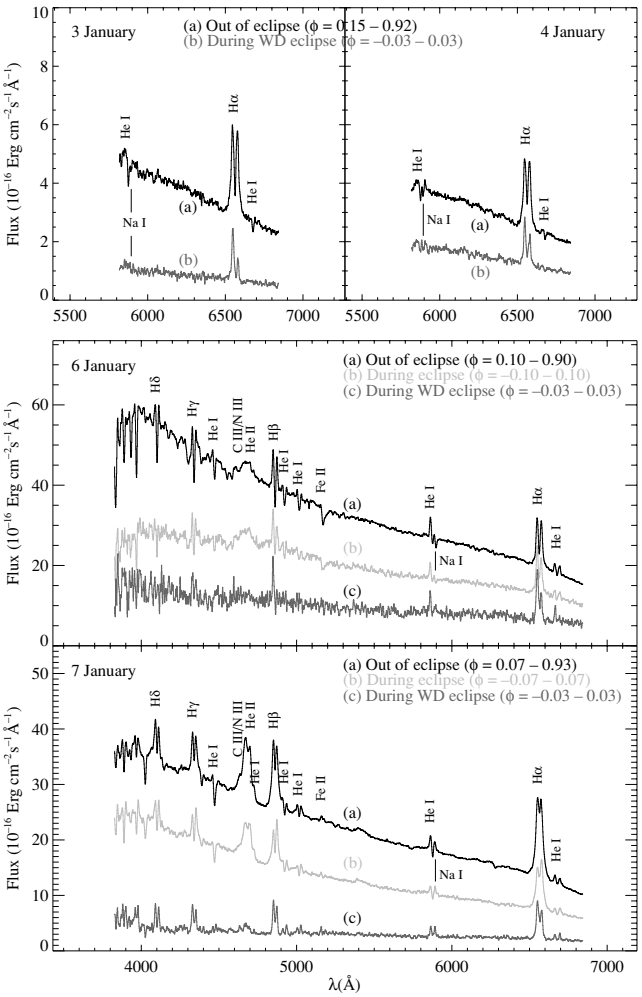

Figure 4. Average spectra of IY UMa during quiescence, rise and normal outburst in 2001 January.

3.2 2001 January: IY UMa rises to normal outburst

Fig. 4 shows the average spectra; for 2001 January 3 and 4 we show just the blue end of the red spectra, which were discussed in Rolfe (2002). The phase ranges used are given in Fig. 4. On 2001 January 3 and 4 the system is quiescent, the only notable difference from 2000 March being the deeper core between the disc peaks.

On 2001 January 6 the system is 7–8 times brighter. Deep core absorption is seen in all emission lines except Hα. This resembles OY Car during a normal outburst (Harlaftis & Marsh 1996) and some superoutburst spectra of Z Cha (Honey et al. 1988). The Balmer absorption wings are no longer seen, meaning that the deep core absorption in outburst cannot be a result of the white dwarf. This also adds weight to the suggestion that the cores in quiescence are not entirely a result of the white dwarf absorption. The 4640 Å C III/N III Bowen blend and He II 4686 Å have appeared, as in IY UMa in superoutburst (Wu et al. 2001), in other dwarf novae in outburst (Morales-Rueda & Marsh 2002) and in nova-likes, e.g. V348 Pup and UX UMa (Tuohy et al. 1990; Rutten et al. 1993; Rolfe 2001). The He II emission probably results from the reprocessing of extreme UV (EUV) and X-ray BL emission (Patterson & Raymond 1985), while the N III emission may come from conversion of He II Lyα transition photons to N III photons via O III (Deguchi 1985).

On 2001 January 7 the continuum is approximately 30 per cent less than January 6 and the line absorption cores are much

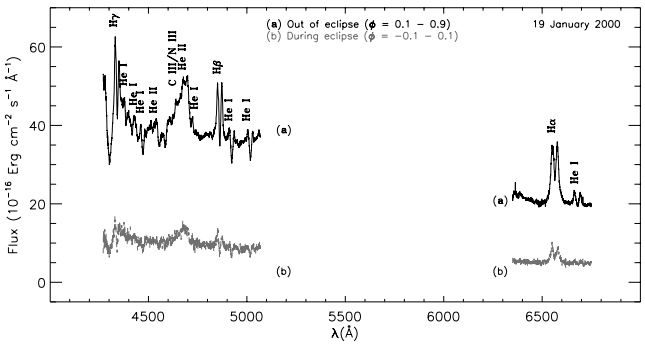

Figure 5. Average spectra of IY UMa during superoutburst.

weaker. He II 4686 Å and the Bowen blend are much stronger, with He II comparable in strength to Hβ. He II 5412 Å is faintly visible. The He II 4686 Å line profile is consistent with strong double-peaked emission from the disc blended with a C III/N III and He I 4713 Å contribution. The most obvious absorption feature is He I 4471 Å. This has low velocity, is very narrow and disappears almost precisely during the white dwarf (WD) eclipses (Fig. 4), implying absorption occurring close to the WD.

IY UMa went into outburst between January 4 and 6, and continued in outburst on January 7. The accretion rate on to the white dwarf must have been several times higher on January 7 than on January 6, increasing the flux of X-rays and EUV emitted from the BL, thus enhancing the strength of the He II emission. Meanwhile the optical continuum decreased between 2001 January 6 and 7, indicating the outer, optical continuum emitting disc was declining from its peak mass accretion rate. This indicates an outside–in outburst. IY UMa returned to quiescence by January 9 or 10 (Steeghs, private communication), suggesting this was a normal outburst.

3.3 2000 January: IY UMa in superoutburst

The average red and blue spectra in Fig. 5 show a variety of hydrogen and helium lines superimposed on a blue continuum. The lines appear double peaked with very deep core absorption: absorption dominates emission in all He I lines except He I 6678 Å. The most striking feature is the emission in He II and the Bowen blend. Bluewards of Hγ is a strong absorption that was also hinted in the 2001 January 6 normal outburst spectra. No such feature was visible on 2001 January 7. The spectrum looks very similar to that during normal outburst on the 2001 January 6, apart from the stronger He II/Bowen emission.

3.4 Equivalent widths

Table 2 gives emission line equivalent widths (EWs) during the two outburst states. These values are from the average out-of-eclipse spectra for each night shown in Figs 4 and 5.

During the 2001 January, normal outburst the EWs of Hα, Hβ and the He II/Bowen/He I blend increase considerably from January 6 to 7, by factors ∼2–4. The EW of Hγ is negative on January 6 as a result of the deep, blue absorption feature. He I 5016 Å is similarly diminished by core absorption on January 6. He I 6678 Å barely changes in EW during the January 2001 observations. During the January 2000 superoutburst, Hα has a similar EW to that on 2001 January 6.

The observations were taken at different stages in two different types of outburst, with the rapidly changing accretion flow leading to complicated changes in the continuum, absorption and emission lines. If irradiation powers the emission lines (cf. Section 3.2) while viscous dissipation produces the continuum, the EW could vary considerably. This is indeed the case for the Balmer lines and He II/Bowen feature, while the absorption dominated He I lines are inconclusive.

Table 2. Equivalent widths (EWs; in Å) of the lines present in the spectra during the two outburst states studied.

	Outburst		Superoutburst
	06/01/01	07/01/01	19/01/00
Hα	23.08±0.14	56.30±0.11	28.54±0.12
Hβ	4.83±0.12	18.19±0.08	9.29±0.09
Hγ	−0.95±0.12	8.77±0.09	11.66±0.12
He I λ5016	0.07±0.09	1.65±0.06	0.72±0.07
He I λ6678	2.72±0.11	2.69±0.08	3.98±0.09
He II 4686 Å +He I λ4713 +Bowenblend	4.82±0.16	22.50±0.11	25.98±0.15

4 LIGHT CURVES

Light curves of the continuum and continuum-subtracted emission lines are shown in Fig. 6 (2000 March) and Fig. 7 (2001 January). Continuum B is the flux integrated in the range 4000–5200 Å (covered by all the March 2000 spectra), while continuum R is over the range 5950–6450 Å (covered by all the 2000 and 2001 spectra except 2000 March 18). For Hβ, the average flux either side of the profile was subtracted to reduce the effect of the absorption wings. Note that slit loss corrections were not possible for the 2000 March observations, but the data suggest that apart from the omitted phase range 2–2.5 on March 18, conditions were photometric. The 2000 January observations conditions were not photometric and no slit loss correction was possible, so we do not present light curves for these data.

4.1 2000 March: quiescence

The continuum light curves for 2000 March reveal the strong orbital hump and eclipse seen in photometry (P2000; Rolfe et al. 2001b). On 2000 March 19 and 20 there is a double-humped structure, with the usual strong orbital hump peaking around phase 0.8–0.9 and a weaker hump peaking around 0.3–0.4. The strong hump is the stream–disc impact coming into view on the near side of the disc, while the weak hump is when the stream–disc impact is again seen roughly length ways, but on the far side of the disc. Similar orbital curves have been seen in WZ Sge and AL Com (Robinson, Nather & Patterson 1978; Patterson et al. 1996), but with both humps having the same amplitude. Hα and Hβ show a stronger secondary hump and a shallower eclipse, the latter resulting from disappearance of the unsubtracted core of the white dwarf Balmer absorption lines during eclipse (an effect that is stronger for Hβ).

4.2 2001 January: normal outburst

The January 3 and 4 continuum curves (Fig. 7) show a single orbital hump; the flux away from hump and eclipse is within a factor ∼2 of 2000 March. The hump is approximately twice as bright on January 3 as on 4. The Hα curve on January 4 shows no sign of the hump. Though low time resolution and phase coverage prevents detailed analysis, we see changes in the behaviour of the system over one day. If it is linked to the following outburst, this is important. No advanced warning of an impending outburst has been seen before.

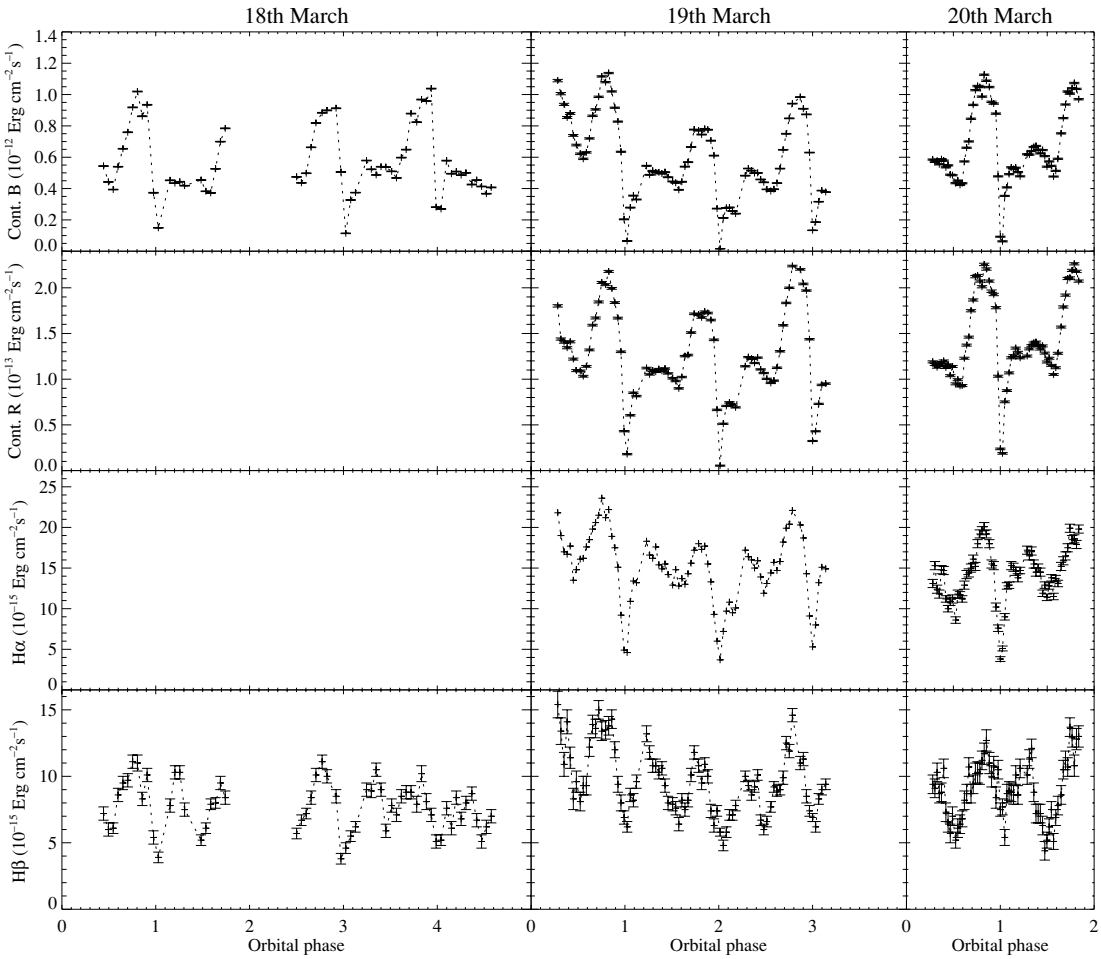

Figure 6. 2000 March quiescence light curves

Between January 4 and 6, the continuum flux rises by a factor of ∼7, decreasing again by the beginning of the observations of January 7. During January 7, the flux drops by a further 20 per cent. The eclipses are all deep, with the eclipse during orbit 42 broader and shallower than those during orbits 55 and 56. This implies the light distribution becomes more concentrated around the white dwarf between January 6 and 7; suggesting the outer disc is returning to quiescence. Measurement by eye yields full eclipse widths that correspond to emission distributions of radius $0.37 \pm 0.10a$ on January 6 shrinking to $0.21 \pm 0.05a$ on January 7. These radii are both much smaller than the 3 : 1 resonance radius ($0.46a$) indicating a normal outburst. NB P2000 measured radius $0.44 \pm 0.03a$ in superoutburst. An unrealistic eccentricity (~ 0.8) is needed for a non-circular disc to explain the change in eclipse width.

The eclipses are fairly symmetrical and centred on phase 0, suggesting emission centred on the white dwarf. In contrast with the continuum, the emission lines all rise on January 6, being nearly twice as bright at the start of the observations on January 7 than during January 6. These changes are not simply a result of variations in the core absorption. The delay in rise of the lines relative to the continuum is between approximately one orbit and two days. On the 2001 January 7, the EWs in Hα and He II increase by approximately 7–8 per cent. The Hα eclipses suggest the same decrease in radius of the line emission region as for the continuum. The Hα EW doubles during eclipse, while for He II it decreases almost to zero. We conclude the He II emission comes from a smaller area than Hα, concentrated closer to the white dwarf.

5 DOPPLER TOMOGRAPHY

Doppler tomography (Marsh & Horne 1988) exploits phase-resolved emission line profiles to produce velocity–space maps of the emission distribution. It assumes the emitting material and its velocities are in the orbital plane, that the brightness and visibility of each point do not vary with phase, and that the intrinsic line profile is narrow compared with the Doppler shifts as a result of the velocity distribution. We excluded data from phases −0.1 to 0.1 because eclipses occur then. The hotspot also has a varying brightness, so Doppler maps indicate only an orbital average of the hotspot emission. The Fourier-filtered back projection technique was used to produce the maps. Levels below the continuum are shown the same as the continuum level.

5.1 2000 March: quiescence

The trailed spectra in 2000 March revealed the same orbital modulation throughout. We therefore consider the phase-folded trails shown in the top row of Fig. 8. Double-peaked emission with eclipse first in the blue peak and then in the red, as expected from a prograde disc, is seen in the Balmer lines. The disc emission in the red wing around phase 0.3 is weaker than at other phases (except eclipse), with this

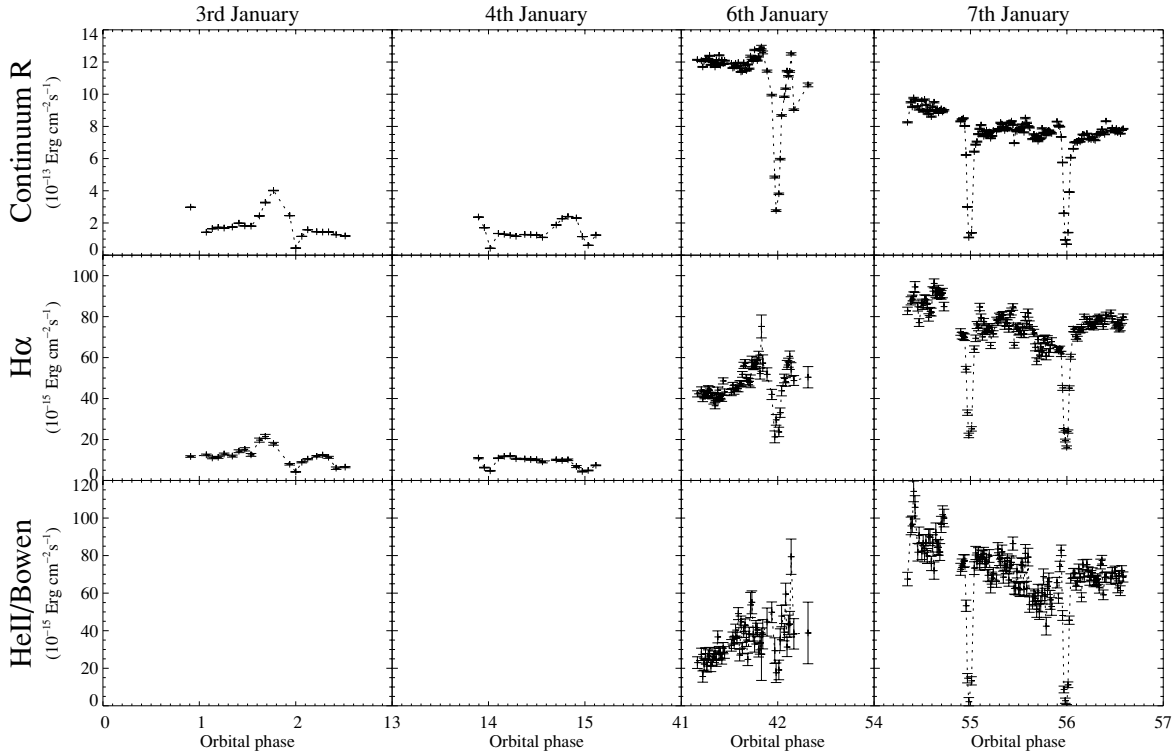

Figure 7. 2001 January light curves during quiescence, rise and normal outburst.

being very clear in Hγ. A similar effect was seen in WZ Sge by Spruit & Rutten (1998), where an *S*-wave of absorption was seen delayed in phase relative to the hotspot *S*-wave. The brightening in the blue wing around phase 0.3 is a distinct feature, not simply the coincidence of the stream and disc emission. This could result from a bright region of the disc on the opposite side from the donor. Between the disc peaks is the core and white dwarf Balmer absorption. A strong *S*-wave with phase-dependent brightness and the same phasing and amplitude appears in all four lines. The strength of the disc emission is similar to that of the *S*-wave emission in Hα, but the relative strength of disc to *S*-wave decreases for higher order Balmer lines, with the brightest parts of the *S*-wave dominating in Hγ. The bottom panel of Fig. 8 shows the trails after subtracting the average line profile in the phase range 0.1–0.9. This removes much of the disc profile and core absorption, revealing that *S*-wave brightness follows that of the orbital hump (cf. Fig. 6). The *S*-wave is eclipsed late indicating an origin at the stream–disc impact. The sharp brightening in the *S*-wave/red wing around phase 0.2 results from poor phase coverage around phase 0.20–0.25 on March 19 and 20.

The four Doppler maps (Fig. 8, row 2) show absorption at low velocity corresponding to the deep cores visible in the average spectra. The Hα map shows emission from disc material within the tidal radius. The stream–disc impact is seen between the two arcs corresponding to the stream trajectory and its Keplerian velocity (cf. U Gem, Marsh 1990 and WZ Sge, Spruit & Rutten 1998). This is also seen in smoothed particle hydrodynamics (SPH) simulations where more detail is apparent (Foulkes et al. 2004). The Hα disc emission is weaker where the two arcs cross it. Spruit & Rutten (1998) point out that the stream–disc impact is hot enough to ionize hydrogen, suppressing Balmer emission until further downstream where the hydrogen has recombined. If the hydrogen in the converging stream and disc flows is ionized, then we expect the Balmer emission from this region to be suppressed. The light curves of Steeghs et al. (2003) suggest that the extreme edge-on inclination of IY UMa affords us a view into a hot shock-heated cavity driven into the disc by the stream impact. SPH simulations (Foulkes et al. 2004) suggest that the dissipation at the impact occurs in both the stream and the disc flows, and is localized at the impact velocity of each. The 2000 March Hα map is suggestive of ionization caused in this way. The $\sim$11 000 K blackbody hotspot temperature found in IY UMa (cf. Fig. 3) would be sufficient to ionize hydrogen.

The third row of Fig. 8 shows the line profiles reconstructed from the Doppler maps, i.e. the line profiles we would see if the emission distribution was exactly as shown in the Doppler map and all assumptions of Doppler tomography were valid. Comparing the reconstructed trails with the observed ones provides a useful measure of how reliable the Doppler maps are. Eclipses (not accounted for in Doppler tomography) are omitted, but we see clearly in the reconstructed trails the same disc and hotspot features as in the observations, but with features resulting from intrinsic variations during the orbit (the hotspot orbital hump) not correctly reproduced, because the Doppler map is an orbital average. The Doppler map has attempted to reproduce the orbital hump by superposing sine waves of differing velocity amplitude. This leads to the emission extending out to $\sim$2000 km s^{-1} at orbital phase 0.5, for which there is no evidence in the observed trails.

5.2 2001 January: normal outburst

In 2001 January, we observed the accretion flow behaviour around the rise from quiescence to normal outburst.

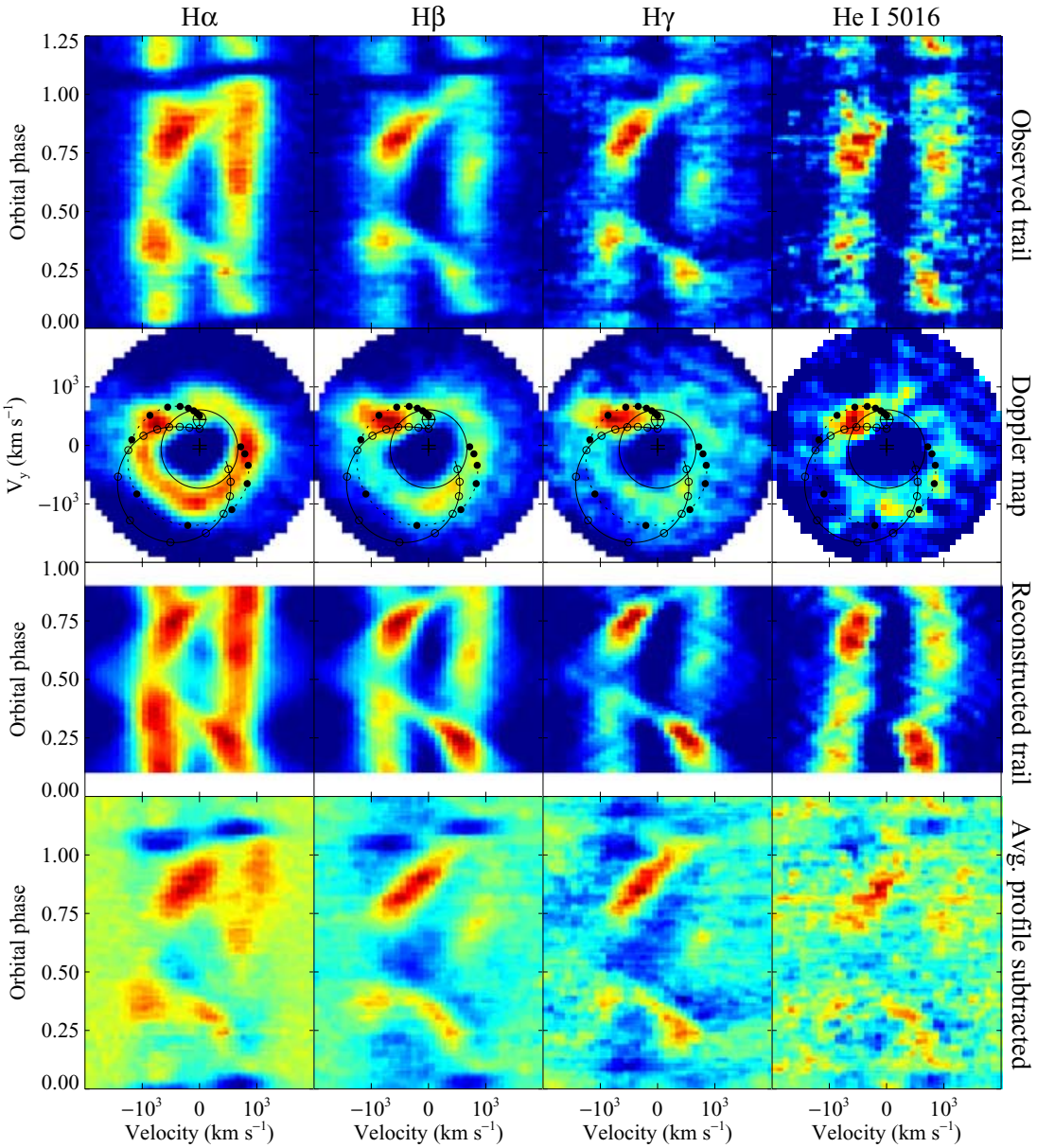

Figure 8. Doppler tomography combining all three nights of data during quiescence in 2000 March. Top row: phase-folded, phase-binned, velocity-binned and continuum-subtracted trailed spectra. Phases 0–0.25 are repeated. Second row: Fourier-filtered back-projections. Emission from the donor star should appear within the black teardrop. Disc emission should appear outside the black circle (the Keplerian velocity at the radius where the disc is tidally truncated). The ballistic stream velocity is the arc with unfilled circles and the arc with filled circles is the Keplerian velocity along the stream trajectory. These markings assume the orbital parameters of P2000. Third row: trailed spectra reconstructed from Doppler maps. Bottom row: observed trail minus average line profile in phase range 0.1 to 0.9.

5.2.1 2001 January 3 and 4: pre-rise

Trailed spectra from 2001 January 3 and 4 for Hα, and He I 5876 Å are shown in Fig. 9. The wavelength of the weak Na I absorption doublet line at 5890–5896 Å corresponds to a velocity range of approximately 700–1000 km s^{-1} relative to He I 5876 Å so we must be wary of this when studying this line. Hα shows double peaks and a blue-to-red eclipse; the *S*-wave is not visible, although brighter regions in the peaks hint at its presence, particularly on 2001 January 4. The low signal-to-noise ratio in He I prevents any structure being seen in that trail, apart from the core/Na I absorption and possibly a bright region around the blue peak between approximately phase 0.6 and 0.75, maybe resulting from an *S*-wave.

Doppler maps for 2001 January 3 and 4 (Fig. 9) are blurred by $\sim$20° by the long exposures and the limited number of spectra. Despite this, all four maps show evidence of the hotspot at the same location as in 2000 March, with He I a little further upstream than the Hα hotspot.

5.2.2 2001 January 6: outburst

The 2001 January 6 Hα, Hβ, Hγ and He I 5016 Å trails (Fig. 10) all show double-peaked disc emission, while the blue-to-red eclipse is seen clearly in Hα and Hβ (the strongest lines). Apart from the rise in brightness throughout the night, there is no other easily identifiable

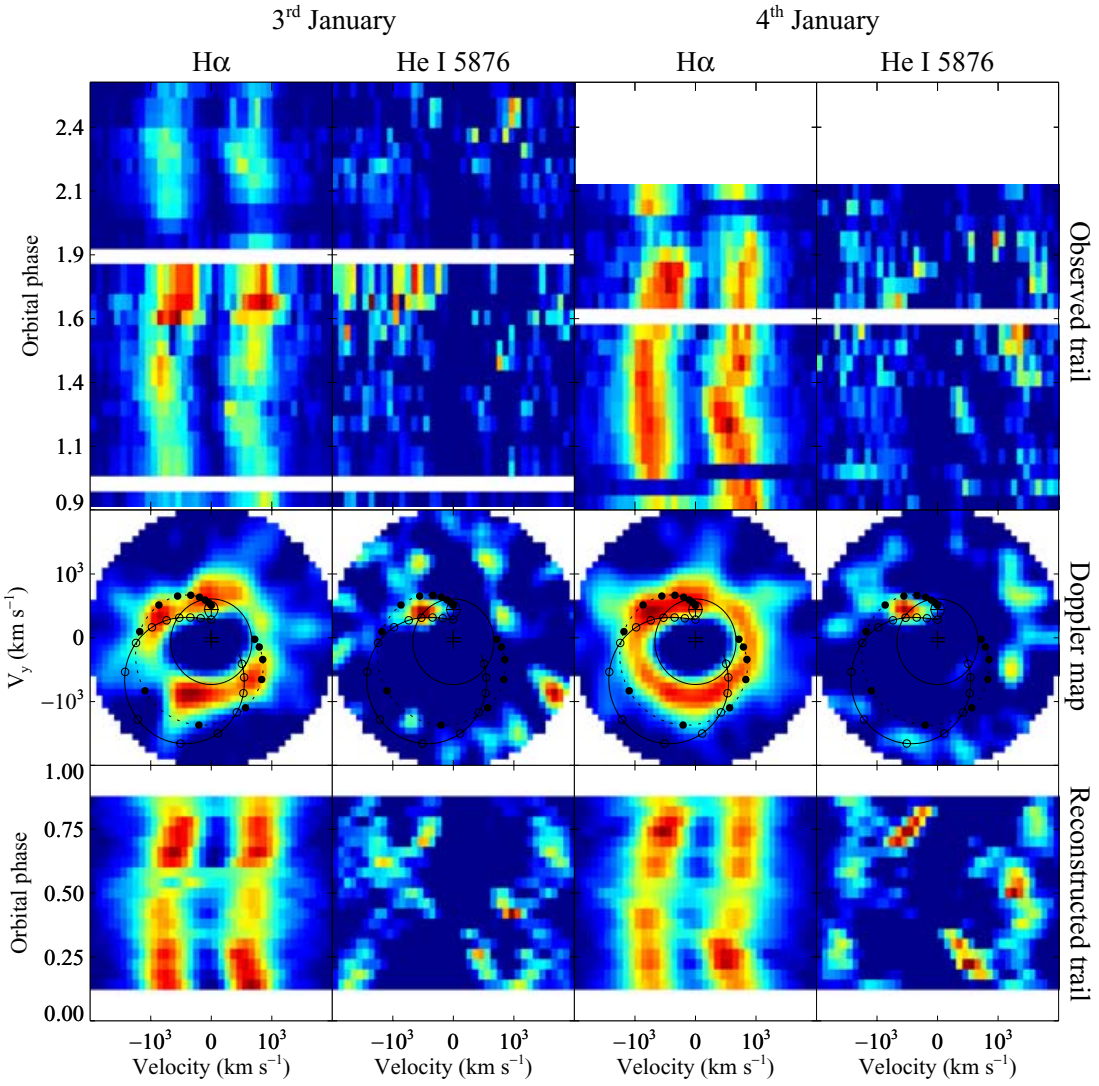

Figure 9. Doppler tomography before outburst in 2001 January. Top row: phase-binned, velocity-binned and continuum-subtracted trailed spectra. Other rows: as in Fig. 8.

behaviour. Deep absorption cores hide any structure between the peaks.

The 2001 January 6 Doppler maps (Fig. 10, second row) differ considerably from those for 2001 January 3 and 4. The Hα map shows a ring of disc emission, which has two bright regions on opposite sides of the disc around maximum and minimum V_y. The same structure is seen in Hβ and Hγ. The He I map is noisier but consistent. The two-fold asymmetry is an artefact from leaving out the eclipse phases: omitting the disc emission during eclipse weakens the left and right sides of the ring in the map, while missing the very strong core absorption during eclipse enhances the strip around $V_x = 0$ in the map, accentuating the top and bottom of the disc ring. The brightening of the line flux during the night (cf. Fig. 7) biases the map and may thus contribute to the two-fold asymmetry. We therefore made a set of maps (Rolfe 2001) using spectra normalized so the total line flux remained constant with time. Hα showed similar asymmetries to those of the maps in Fig. 10, while the other lines produced inferior maps as a result of the effects of noise in the integrated line flux. Accordingly, we conclude the maps from 2001 January 6 show no more than emission from a disc within the tidal radius.

Each map for 2001 January 6 had its azimuthally averaged map subtracted (Fig. 10, third row), enhancing non-axisymmetric features. This removes much of the disc ring and the central absorption. The Balmer maps clearly show emission coming from the velocity of the donor star. The quality of the He I map is too poor to identify or rule out such a feature. The reconstructed trails show clearly the disc emission and core absorption, with the double peaks disappearing around phase 0.5 in contradiction with the observations, confirming the conclusion that the asymmetry in the Doppler maps is an artefact of omitting eclipses.

We subtracted the average line profiles for the phase range 0.2–0.8 from the observed trails (Fig. 10, bottom row), reducing the disc and absorption components. Overplotted is the expected velocity of the donor star. There is clear evidence of a weak emission component in Hα following the donor velocity. This confirms that there is emission from the donor velocity and that this is not merely an artefact in the Doppler maps, at least in the case of Hα.

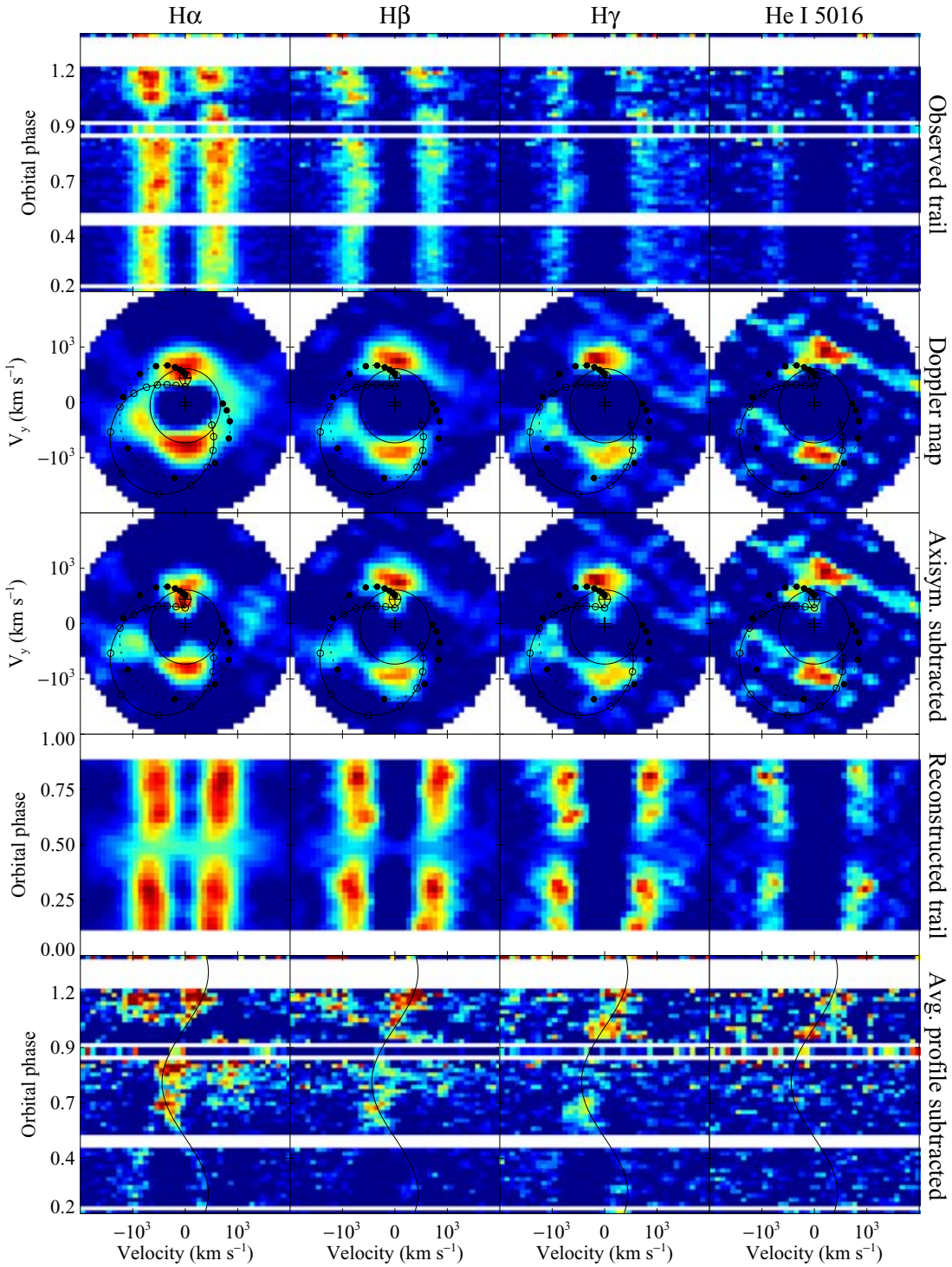

Figure 10. Doppler tomography during rise/normal outburst on 2001 January 6. Top, second and fourth row: as in Fig. 9. Third row: non-axisymmetric component of Doppler maps in second row. Bottom row: observed trail minus average line profile in phase range 0.2 to 0.8, with donor velocity overplotted.

5.2.3 2001 January 7: decline

The Balmer trails on 2001 January 7 (Fig. 11) reveal more complicated structure than on 2001 January 6 because the absorption cores are substantially weaker. The behaviour is stable throughout the night and is the same for all four lines, except that the core is deeper for higher-order lines. There are double peaks and the clear blue-to-red eclipse. There is a clear *S*-wave with velocity semi-amplitude $\sim$300–600 km s^{-1} and maximum redshift around phase 0.25, disappearing from approximately phase -0.2 to 0.2. This *S*-wave appears to originate on the inner face of the donor star. The velocity, phasing and invisibility at phase -0.2 to 0.2 all suggest this, cf. IP Peg during outburst, e.g. Morales-Rueda, Marsh & Billington (2000).

The trails suggest another *S*-wave. In the blue disc wing around phase 0.4 centred on a velocity of approximately -700 km s^{-1}, we see a bright region that covers a phase range of less than 0.1 and

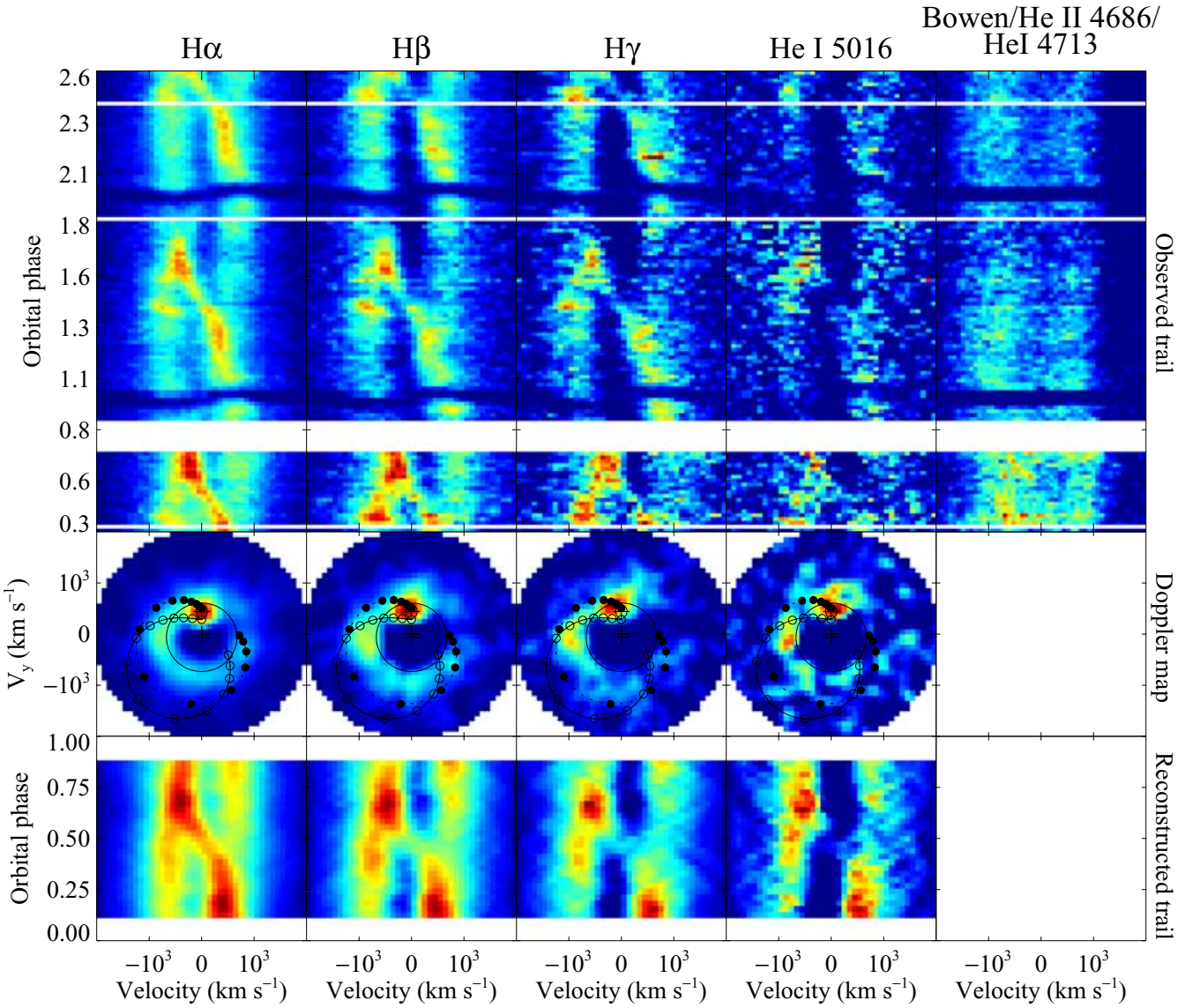

Figure 11. Doppler tomography during normal outburst on 2001 January 7. Rows as in Fig. 9.

a velocity range of more than 500 km s^{-1}. This is seen in all three orbits in Hα and Hβ, and can also be seen more faintly in Hγ and He I. In the first orbit in the red wing at phase 0.9 we see a similar feature at a velocity of approximately 700 km s^{-1}, probably the opposite extremum of the same *S*-wave, but much fainter, cf. OY Car (Harlaftis & Marsh 1996).

The middle row of Fig. 11 shows the Doppler maps for January 7. The Balmer and He I 5016 Å maps show strong emission concentrated around the velocity of the donor star, confirming our inference from the trails and less directly from the maps from the previous night. Given the resolution, this source is consistent with emission from the inner face of the donor. Emission from the donor star during outburst has been seen before, e.g. OY Car (Harlaftis & Marsh 1996) and IP Peg (Marsh 1990; Morales-Rueda et al. 2000; Steeghs 2001). Irradiation-driven He II 4686 Å emission was present in these systems, as in IY UMa (Fig. 11). Marsh (1990) and Harlaftis & Marsh (1996) concluded that EUV emission and X-ray emission from the BL could drive the Balmer emission. The Balmer emission in IY UMa is correlated with He II (Fig. 7), suggesting the same driving mechanism.

The other notable feature seen in the January 7 maps is an arc of emission on the left hand side (negative V_x) at velocities corresponding to the outer part of the disc. We do not see the full circle corresponding to the whole disc. The arcs are brightest around $V_y = 0$. In Hα and Hβ, the arc stretches through approximately 270° (measured anticlockwise from the donor velocity), while in Hγ and He I it only reaches approximately 135°, although He I shows a bright blob around 225°. This structure appears similar to that seen in outburst in OY Car by Harlaftis & Marsh (1996), which followed and was thus attributed to the accretion stream. However, in IY UMa this is not the case; it follows the velocity of the outer disc and no stream–disc impact hotspot is seen, so this emission does not arise from dissipation of energy where the stream hits the disc edge. Despite the lack of emission from dissipation of kinetic energy at the stream–disc impact, some vertically extended structure is likely to be present where the stream impacts the disc, providing a

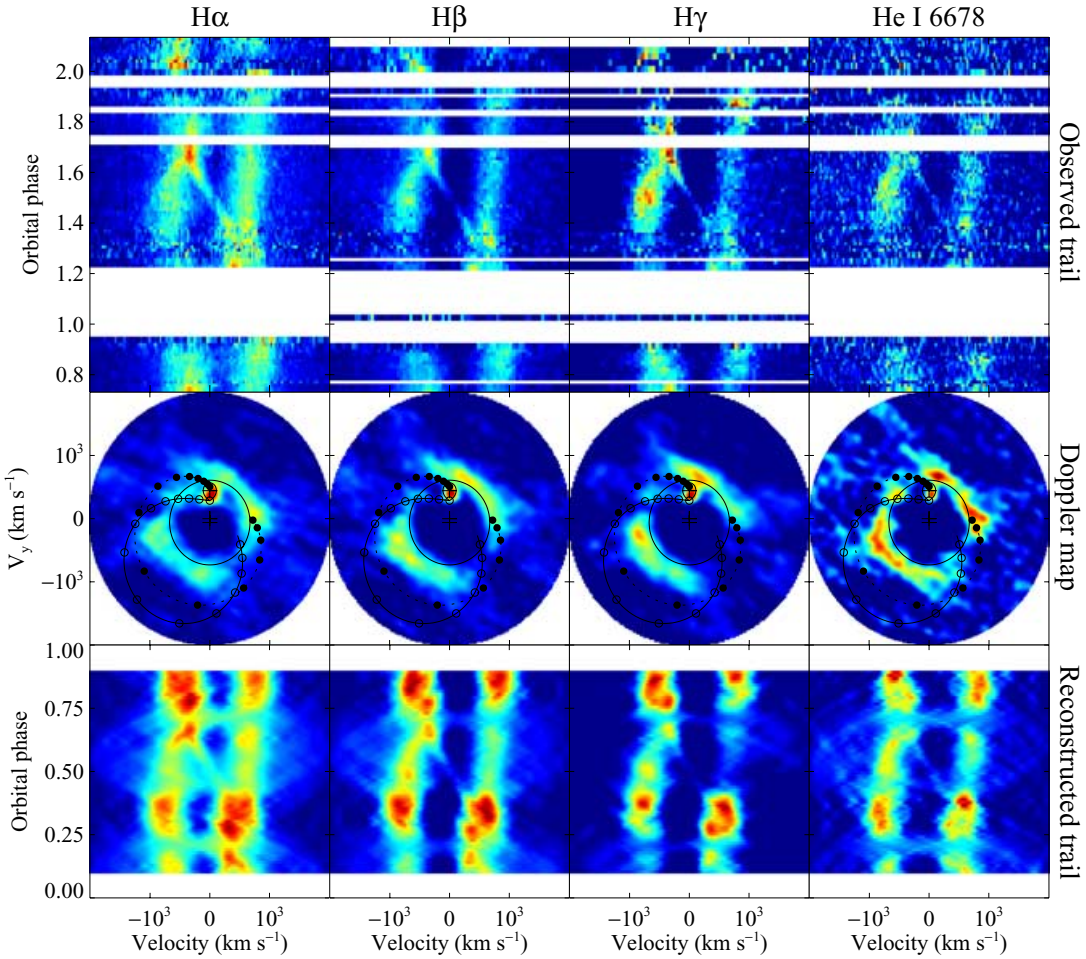

Figure 12. Doppler tomography during superoutburst on 2000 January 19. Rows as in Fig. 9.

region where we might see reprocessing of the EUV and X-rays from the BL, simply because vertically extended structure will intercept more BL radiation. This would be top left in the Doppler maps. If this vertical structure, raised at this point initially by the stream disc impact, extended further around the disc, it could explain the brightest region of the emission line arcs seen here. The inner face of this raised region should appear bright, being directly irradiated, explaining why the corresponding feature in the trailed spectrogram is brighter when we look at the inner face (phase ∼0.4) than the outer face (phase ∼0.9). Simulations of discs and the stream–disc impact do show vertical structure extended around the disc edge, e.g. Hirose, Osaki & Mineshige (1991) and Armitage & Livio (1996), and there is much observational evidence for vertical structure in the outer disc and a flared disc during outburst (e.g. Naylor et al. 1987; Billington et al. 1996; Ioannou et al. 1999). If the core absorption in the lines is the result of material in the outer disc along the line of sight to the white dwarf, then the weakening of the core absorption on January 7 points towards changes in the vertical structure of the outer disc. Such changes might reveal vertical structure around the hotspot on January 7, which was entirely swamped by a uniformly thick outer disc on January 6. We expect some reprocessing of the light from the BL throughout the disc, which could explain why the ring extends most, if not all, of the way around the disc in the Hα and Hβ maps. We conclude that the structure in the January 7 maps can be explained by reprocessing of BL EUV and X-ray emission on the inner face of the donor and vertical structure in the disc near to and perhaps triggered by the stream–disc impact.

The reconstructed Balmer and He I trails are consistent with those observed, showing the double peaks, deep core and donor *S*-wave. The feature around phase 0.4 in the blue wing is smeared out but identifiable.

5.3 2000 January: superoutburst

We normalized the line profiles by scaling each so that the integrated line flux above the continuum was the same for all. This reduced the variability in the flux caused by poor observing conditions. These normalized trailed spectra for 2000 January 19 (Fig. 12, top row) show the double-peaked structure characteristic of accretion discs. Also present in all lines is the deep core between the disc peaks, which is below the continuum except in Hα. The Balmer lines and He I 6678 Å show a narrow partial *S*-wave that moves from red (phase 1.3) to blue (phase 1.7) and disappears around phase 1.8. This looks like the donor star emission seen during the normal outburst but not during quiescence. We see the inner face of the donor star only during the two bright states, supporting the idea that the donor star is being irradiated. The Doppler maps (middle row of Fig. 12) all show disc emission with asymmetric artefacts like those on 2001 January 6, which resulted from incomplete phase

coverage. The donor emission is visible in these maps. The asymmetry probably results from the incomplete phase coverage, though during superoutburst the disc is tidally distorted and precessing, and so asymmetric dissipation patterns and vertical structure in the disc are expected (e.g. Foulkes et al. 2004). The reconstructed Balmer and He I trails show bright red-shifted emission around phase 0.3 and blue-shifted emission around 0.8. This is the donor *S*-wave crossing the disc peaks, and is not seen in the observed trails because the inner face of the donor will be only half visible at phases 0.25 and 0.75, and is completely invisible around phase 0.

6 DISCUSSION

There are several sets of photometry of eclipsing dwarf novae beginning early during the rise to outburst. Vogt (1983) presents the rise to a normal outburst of OY Car, while Webb et al. (1999) presents an entire outburst of IP Peg. Ioannou et al. (1999) presents observations of another short-period high-inclination dwarf nova, HT Cas, covering the rise, peak and decline from a normal outburst. Vogt (1983) and Rutten et al. (1992) showed that during the rise to outburst in OY Car, the outer disc rapidly brightens (as it enters the hot ionized state), with this hot bright region quickly propagating inwards towards the white dwarf, the outer radius remaining constant. As the outburst reaches maximum brightness, the radius of the emission region shrinks by approximately a third. Ioannou et al. (1999) find exactly the same outside–in behaviour in HT Cas, additionally concluding that the disc becomes vertically flared during outburst. In IY UMa, the emission region shrinks and the eclipse depth increases between the observed continuum maximum and a day later. This indicates the outer disc returns to quiescence before the inner disc, as the cooling wave propagates inwards. The disc emission region shrinks during decline in most (if not all) dwarf novae, including two dwarf novae where eclipses suggested an outburst beginning in the inner disc and propagating outwards (IP Peg and EX Dra; Webb et al. 1999 and Baptista & Catalán 2001, respectively). Eclipse light curves at the very start of the outburst are required to distinguish between inside–out and outside–in outbursts from single-band photometry alone.

The apparent disappearance of the orbital hump in Hα on 2001 January 4 immediately preceding the normal outburst while there is still hotspot line emission seen in the Doppler map is curious. It must result from a change in geometry of the hotspot making it equally visible at all phases. This may simply be the result of the inherent variability in the stream–disc impact and disc structure, but we note that while the amplitude of the hotspot is variable, none of our other observations show it completely disappearing. The disappearance may be the result of a change in the structure of the outer disc as the outburst begins. This would require the outburst to begin in the outer disc, so that there has been no increase in luminosity detected when it occurs.

The delay in the rise of the line emission compared with the rise of the continuum is something that can only be detected in rare (and fortuitous) spectrophotometry in the earliest stages of outburst like those analysed here. The delay is easily understood if the line emission in outburst is powered by irradiation from the BL and the outburst is of the outside–in type seen in OY Car and HT Cas. The viscous dissipation-powered continuum begins to rise as soon as the outer disc enters the high state, while the emission lines do not become significantly stronger until the heating wave has reached the inner disc increasing the intensity of high energy BL emission and the emission lines it powers. This delay of the lines relative to the continuum is analogous to the UV delay in dwarf nova outburst observations (Wheatley, Mauche & Mattei 2003), where the UV emission (from the inner disc) rises after the visual emission, which comes predominantly from the outer disc. The strong He II emission, thought to be powered by irradiation, the Balmer light curves mimicking that of He II, the emission from the inner face of the donor star and the phase-dependent arc of emission in the 2001 January 7 lines all support the conclusion that the emission lines are predominantly powered by irradiation during outbursts.

7 SUMMARY

Extensive spectroscopic observations of IY UMa have revealed classic quiescent accretion flow, with:

(i) strong continuum and line emission from the hotspot region;
(ii) a blackbody hotspot temperature of $\sim$11 000 K;
(iii) ionization of hydrogen in the hotspot region suppressing Balmer emission from the disc close to the hotspot.

Rare spectrophotometry of the rise to a normal outburst reveals:

(i) the continuum and line emission regions shrink at the outburst peak;
(ii) the rise in emission line flux is delayed relative to the continuum by a few hr to 2 d;
(iii) during outburst Balmer, He II and Bowen blend emission is seen from the disc, while Balmer emission is also seen from the inner face of the donor and possible vertical structure in the outer disc.

We conclude that the 2001 January outburst was of the outside–in type, beginning in the outer disc and propagating inwards. Irradiation by EUV and X-rays from the BL powers the emission lines during outburst, with the time taken for mass to move inwards during the outburst explaining the delay between the rise of the continuum and emission line flux.

ACKNOWLEDGMENTS

The data presented here have been taken using ALFOSC, which is owned by the Instituto de Astrofisica de Andalucia (IAA) and operated at the NOT under agreement between IAA and the NBIfAFG of the Astronomical Observatory of Copenhagen. The NOT is operated on the island of La Palma jointly by Denmark, Finland, Iceland, Norway and Sweden, in the Spanish Observatorio del Roque de los Muchachos of the Instituto de Astrofisica de Canarias. The WHT is operated on the island of La Palma by the Isaac Newton Group in the Spanish Observatorio del Roque de los Muchachos of the Instituto de Astrofísica de Canarias. DJR was supported by a PPARC studentship and the Open University (OU) research committee and by a PPARC rolling grant at Leicester. CAH gratefully acknowledges support from the Leverhulme Trust F/00-180/A. LMR was supported by a PPARC post-doctoral grant. The authors gratefully acknowledge the work of the VSNET (http://www.kusastro.kyoto-u.ac.jp/vsnet/index.html). The reduction and analysis of the WHT data were carried out on the Southampton node of the Starlink network. The authors thank Rob Hynes for useful comments.

REFERENCES

Armitage P. J., Livio M., 1996, ApJ, 470, 1024
Baptista R., Catalán M. S., 2001, MNRAS, 324, 599
Billington I., Marsh T. R., Horne K., Cheng F. H., Thomas G., Bruch A., O'Donoghue D., Eracleous M., 1996, MNRAS, 279, 1274

Deguchi S., 1985, ApJ, 291, 492
Foulkes S. B., Haswell C. A., Murray J. R., Rolfe D. J., 2004, MNRAS, 349, 1179
Harlaftis E. T., Marsh T. R., 1996, MNRAS, 308, 97
Hessman F. V., Koester D., Schoembs R., Barwig H., 1989, A&A, 213, 167
Hirose M., Osaki Y., Mineshige S., 1991, PASJ, 43, 809
Honey W. B., Charles P. A., Whitehurst R., Barrett P. E., Smale A. P., 1988, MNRAS, 231, 1
Ioannou Z., Naylor T., Welsh W. F., Catalán M. S., Worraker W. J., James N. D., 1999, MNRAS, 310, 398
Marsh T. R., 1989, PASP, 101, 1032
Marsh T. R., 1990, ApJ, 349, 593
Marsh T. R., Horne K., 1988, MNRAS, 235, 269
Marsh T. R., Horne K., Shipman H. L., 1987, MNRAS, 225, 551
Marsh T. R., Horne K., Schlegel E. M., Honeycutt R. K., Kaitchuck R. H., 1990, ApJ, 364, 637
Morales-Rueda L., Marsh T. R., 2002, MNRAS, 332, 814
Morales-Rueda L., Marsh T. R., Billington I., 2000, MNRAS, 313, 454
Naylor T., Charles P., Hassal B., Bath G. T., Berriman G., Warner B., Bailey J., Reinsch K., 1987, MNRAS, 229, 183
Osaki Y., 1996, PASJ, 108, 39
Osaki Y., Meyer F., 2003, A&A, 401, 325
Patterson J., Raymond J. C., 1985, ApJ, 292, 550
Patterson J., Augusteijn T., Harvey D. A., Skillman D. R., Abbott T. M. C., Thorstensen J., 1996, PASP, 108, 748
Patterson J., Kemp J., Jensen L., Vanmunster T., Skillman D.R., Martin B., Fried R., Thorstensen J. R., 2000, PASP, 112, 1567 (P2000)
Robinson E. L., Nather R. E., Patterson J., 1978, ApJ, 219, 168
Robinson E. L. et al., 1995, ApJ, 443, 295
Rolfe D. J., 2001, PhD thesis, The Open Univ.
Rolfe D. J., 2002, MNRAS, 334, 699
Rolfe D. J., Abbott T. M. C., Haswell C. A., 2001a, Lecture Notes in Phys., 573, 39
Rolfe D. J., Haswell C. A., Patterson J., 2001b, MNRAS, 324, 529
Rolfe D. J., Abbott T. M. C., Haswell C. A., 2002, in Gänsicke B., Beuermann K., Reinsch K., eds, in ASP Conf. Ser., The Physics of Cataclysmic Variables and Related Objects. Astron. Soc. Pac., San Francisco, p. 537
Rutten R. G. M., Kuulkers E., Vogt N., van Paradijs J., 1992, A&A, 265, 159
Rutten R. G. M., Dhillon V. S., Horne K., Kuulkers E., van Paradijs J., 1993, Nat, 362, 518
Spruit H. C., Rutten R. G. M., 1998, MNRAS, 299, 768
Stanishev V., Kraicheva Z., Boffin H. M. J., Genkov V., 2001, A&A, 367, 273
Steeghs D., 2001, Lecture Notes in Phys., 573, 45
Steeghs D., Perryman M. A. C., Reynolds A., de Bruijne J. H. J., Marsh T., Dhillon V. S., Peacock A., 2003, MNRAS, 339, 810
Tuohy I., Remillard R., Bradt H. V., Brissenden R., 1990, ApJ, 359, 204
Vogt N., 1983, A&A, 128, 29
Webb N. A. et al., 1999, MNRAS, 310, 407
Wheatley P., Mauche C., Mattei J., 2003, MNRAS, 345, 49
Wood J. H., Horne K., Berriman G., Wade R., O'Donoghue D., Warner B., 1986, MNRAS, 219, 629
Wu X., Li Z., Gao W., Leung K.-C., 2001, ApJ, 549, L81

This paper has been typeset from a TEX/LATEX file prepared by the author.